Copyright © 2011 Tech Science Press CMES, vol.78, no.4, pp.209-224, 2011

Application of the OMLS Interpolation to Evaluate Volume Integrals Arising in Static Elastoplastic Analysis via BEM

K.I. Silva[1], **J.C.F. Telles**[2] **and F.C. Araújo**[3]

Abstract: In this work the boundary element method is applied to solve 2D elastoplastic problems. In elastoplastic boundary element analysis, domain integrals have to be calculated to introduce the contribution of yielded zones. Traditionally, the use of internal integration cells have been adopted to evaluate such domain integrals. The present work, however, proposes an alternative cell free strategy based on the OMLS (Orthogonal Moving Least Squares) interpolation, typically adopted in meshless methods. In this approach the definition of points to compute the interpolated value of a function at a given location only depends on their relative distance, without need to define any element or cell connectivity. In addition, a criterion–independent explicit procedure has been used for analyzing the inelastic non–linear problem. Analyses of existing problems found in the literature are used to illustrate the accuracy of the proposed technique.

Keywords: Boundary Element Method, Elastoplasticity, Orthogonal Moving Least Squares Interpolation, Meshless methods.

1 Introduction

In elastoplastic analysis via the boundary element method (BEM), domain discretization, usually by means of integration cells, is naturally needed to take into account the residual stresses in yielded zones of the solid [Brebbia, Telles, and Wrobel (1984); Telles (1983); Telles and Carrer (1991)].

In the present work a different alternative is explored. The strategy is based on the application of the OMLS (orthogonal moving least squares) interpolation, typically used to develop meshless methods, to approximate the domain integrals arising from plastic terms in the BEM formulation. In other words, the idea here has been

[1] UFSJ, Ouro Branco, MG, Brazil - katia@ufsj.edu.br
[2] UFRJ, Rio de Janeiro, RJ, Brazil - telles@coc.ufrj.br
[3] UFOP, Ouro Preto, MG, Brazil - fcelio@em.ufop.br

to remove standard domain cell discretization to compute the domain integrals, leading to a simpler and perhaps more elegant viable procedure.

The OMLS strategy is derived from the MLS (moving least squares) method, according to which a function value to be reconstructed at a certain point of its definition domain only depends on the distance from this point to the points contributing to that particular function value. Nevertheless, unlike the MLS method, in the OMLS approach orthogonal weighting functions are used as basis functions, what causes the resulting approximation function to have a delta–distribution characteristic, and allows for working with real values of the physical quantities to be interpolated. Furthermore, the system of equations obtained for determining the OMLS interpolation parameters is well–conditioned and, compared to the MLS method, less coefficients are employed in the process [Atluri and Zhu (2000); Atluri and Shen (2002, 2005); Liew, Cheng and Kitipornchai (2006)].

By applying the OMLS strategy, plastic effects are included into the regular algebraic BE system of equations with no need for integration cells. To illustrate the accuracy of the technique proposed, elastoplastic results of three numerical examples are presented using OMLS–based and cell–based BEM techniques, including some comparisons to finite element solutions.

2 BEM formulation for elastoplastic problems

The integral equations for expressing displacement and stress components in elastoplastic problems via the BEM are given (body forces are neglected) as

$$\begin{aligned} & c_{ij}(\xi)\,\dot{u}_j(\xi) + \int_\Gamma p^*_{ij}(\xi,\mathbf{x})\,\dot{u}_j(\mathbf{x})\,d\Gamma(\mathbf{x}) = \\ & \int_\Gamma u^*_{ij}(\xi,\mathbf{x})\,\dot{p}_j(\mathbf{x})\,d\Gamma(\mathbf{x}) + \int_\Omega \varepsilon^*_{jki}(\xi,\mathbf{x})\,\dot{\sigma}^p_{jk}(\mathbf{x})\,d\Omega(\mathbf{x}) \end{aligned} \tag{1}$$

$$\begin{aligned} \dot{\sigma}_{ij}(\boldsymbol{\xi}) = & \int_\Gamma u^*_{ijk}(\boldsymbol{\xi},\mathbf{x})\,\dot{p}_k(\mathbf{x})\,d\Gamma(\mathbf{x}) - \int_\Gamma p^*_{ijk}(\boldsymbol{\xi},\mathbf{x})\,\dot{u}_k(\mathbf{x})\,d\Gamma(\mathbf{x}) + \\ & + \int_\Omega \varepsilon^*_{ijkl}(\xi,\mathbf{x})\,\dot{\sigma}^p_{kl}(\mathbf{x})\,d\Omega(\mathbf{x}) + g_{ij}\left(\dot{\sigma}^p_{kl}\right) \end{aligned} \tag{2}$$

where Ω represents the domain of the body, Γ its boundary and c_{ij} is the free coefficient found in elastic analysis.

In Eq. 1 u^*_{ij}, p^*_{ij} and ε^*_{jki} are, respectively, the displacement, traction and strain components at point $\mathbf{x}$ due to a unit concentrated load applied in i direction at point $\boldsymbol{\xi}$, i.e., the fundamental solutions of the problem. $\dot{u}_j$, $\dot{p}_j$ and $\dot{\sigma}^p_{jk}$ are the displacement, traction and fictitious "plastic stress" increments of the problem.

It is worth mentioning that, in Eq. 2, the domain integral of the fictitious "plastic stress" is a Cauchy principal value integral and the free term, g_{ij}, results from the derivative of the domain integral present in Eq. 1 [Telles (1983, 1985)].

In general, the numerical solution of the integral equations 1 and 2 is carried out by interpolating the field variables at hand by means of boundary elements and domain cells so as to convert these equations into an algebraic system of equations. Unlike previous approaches, however, in this work the OMLS technique is employed to substitute the internal cell interpolation for the evaluation of such domain integrals.

3 3 Orthogonal Moving Least–Squares (OMLS)

In the OMLS approach, the approximation of a function $u(\mathbf{x})$, $\mathbf{x} \in \Omega$ (its definition domain), is based on its OMLS definition domain, Ω_x, which is defined by the set of points $\mathbf{x}_i$, $i = 1, 2, \cdots, n$, wherein n is the number of points in Ω that contribute to the interpolation of $u(\mathbf{x})$ (see Fig. 1).

The OMLS approximation is expressed by

$$u^h(\mathbf{x}) = \bar{\Phi}(\mathbf{x})\ \mathbf{u} \tag{3}$$

where $\mathbf{u}$ is a vector containing the real quantities to be interpolated, and $\bar{\Phi}(\mathbf{x}) = \bar{\mathbf{p}}^T(\mathbf{x})\bar{\mathbf{A}}^{-1}(\mathbf{x})\bar{\mathbf{B}}(\mathbf{x})$ is a vector containing the OMLS interpolation functions, also

$$\bar{\mathbf{A}}(\mathbf{x}) = \bar{\mathbf{P}}^T\mathbf{W}(\mathbf{x})\bar{\mathbf{P}} \tag{4}$$

$$\bar{\mathbf{B}}(\mathbf{x}) = \bar{\mathbf{P}}^T\mathbf{W}(\mathbf{x}) \tag{5}$$

$$\bar{\mathbf{P}} = \begin{Bmatrix} \bar{\mathbf{p}}^T(\mathbf{x}_1) \\ \bar{\mathbf{p}}^T(\mathbf{x}_2) \\ \vdots \\ \bar{\mathbf{p}}^T(\mathbf{x}_n) \end{Bmatrix} \tag{6}$$

and

$$\mathbf{W} = \begin{bmatrix} w(\mathbf{x}-\mathbf{x}_1) & 0 & \cdots & 0 \\ 0 & w(\mathbf{x}-\mathbf{x}_2) & \cdots & 0 \\ \vdots & \vdots & \ddots & \vdots \\ 0 & 0 & \cdots & w(\mathbf{x}-\mathbf{x}_n) \end{bmatrix}_{n\times n} \tag{7}$$

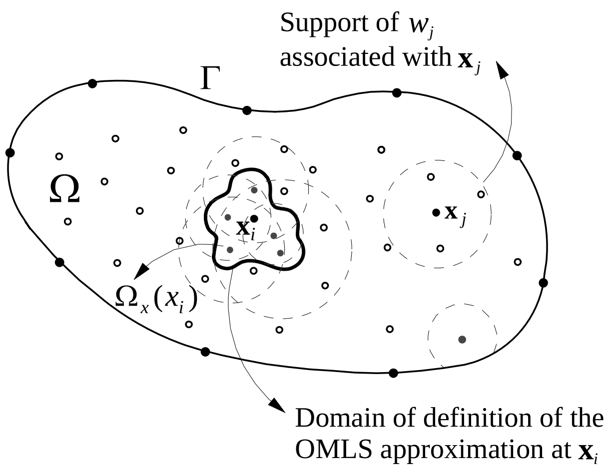

Figure 1: Domain of definition and support of weight function

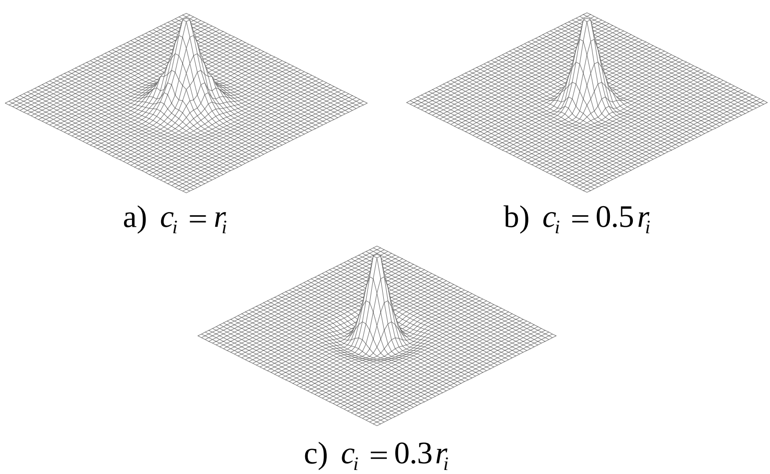

Figure 2: Gaussian weighting function

In the expressions above, $w_i(\mathbf{x}) = w(\mathbf{x}-\mathbf{x}_i)$ is the weighting function associated with the $\mathbf{x}_i$ point, which has the following characteristics: its support, $S[w_i(\mathbf{x})]$, is radial with radius r_i (see Fig. 1), and $0 < w_i(\mathbf{x}) \leq 1$ for all $\mathbf{x} \in S[w_i(\mathbf{x})]$. In this work, the Gaussian function

$$w(\mathbf{x}-\mathbf{x}_i) = \begin{cases} \dfrac{e^{-\left(\frac{d_i}{c_i}\right)^2} - e^{-\left(\frac{r_i}{c_i}\right)^2}}{1-e^{-\left(\frac{r_i}{c_i}\right)^2}}, & 0 \leq d_i \leq r_i \\ 0, & d_i \geq r_i \end{cases} \tag{8}$$

is employed as the weighting function, where $d_i = |\mathbf{x}-\mathbf{x}_i|$ and c_i is a constant that controls the shape of $w(\mathbf{x}-\mathbf{x}_i)$ (Fig. 2).

The other function in Eq. 6, $\bar{\mathbf{p}}(\mathbf{x})$, is the interpolation basis, which is composed by a set of polynomials, mutually orthogonal with regard to the weighting functions, derived from a monomial basis $\mathbf{p}(\mathbf{x})$ by applying the Gram–Schmidt orthogonalization process [Kreider, Kuller, Ostberg, and Perkins (1966)]. For 2D problems, the following bases are usually considered:

$$\mathbf{p}^T(\mathbf{x}) = (1, x_1, x_2), \text{ linear basis} \tag{9a}$$

$$\mathbf{p}^T(\mathbf{x}) = \left(1, x_1, x_2, x_1^2, x_1 x_2, x_2^2\right), \text{ quadratic basis} \tag{9b}$$

Using the OMLS interpolation, equations 1 and 2 are expressed in discretized form as

$$\begin{aligned} & c_{ij}(\boldsymbol{\xi})\,\dot{u}_i(\boldsymbol{\xi}) = \\ & -\sum_{l=1}^{ne}\left(\int_{\Gamma_l} p_{ij}^*[\boldsymbol{\xi}, x(\eta)] \sum_{q=1}^{nnoel} h_q(\eta)\, d\Gamma[x(\eta)]\right)\dot{u}_{jq}^{(l)} + \\ & + \sum_{l=1}^{ne}\left(\int_{\Gamma_l} u_{ij}^*[\boldsymbol{\xi}, x(\eta)] \sum_{q=1}^{nnoel} h_q(\eta)\, d\Gamma[x(\eta)]\right)\dot{p}_{jq}^{(l)} + \\ & + \sum_{d=1}^{NT}\left(\int_{\Omega_d} \varepsilon_{jki}^*(\boldsymbol{\xi}, \mathbf{x}) \sum_{I=1}^{n} \bar{\Phi}_I(\mathbf{x})\, \dot{\sigma}_{jk}^p(\mathbf{x}_I)\, d\Omega_d(\mathbf{x})\right) \end{aligned} \tag{10}$$

$$
\begin{aligned}
&\dot{\sigma}_{ij}(\boldsymbol{\xi}) = \\
&-\sum_{l=1}^{ne}\left(\int_{\Gamma_l} p^*_{ijk}\left[\boldsymbol{\xi},x(\eta)\right]\sum_{q=1}^{nnoel} h_q(\eta)\, d\Gamma\left[x(\eta)\right]\right)\dot{u}^{(l)}_{kq}+ \\
&+\sum_{l=1}^{ne}\left(\int_{\Gamma_l} u^*_{ijk}\left[\boldsymbol{\xi},x(\eta)\right]\sum_{q=1}^{nnoel} h_q(\eta)\, d\Gamma\left[x(\eta)\right]\right)\dot{p}^{(l)}_{kq}+ \\
&+\sum_{d=1}^{NT}\left(\int_{\Omega_d} \varepsilon^*_{ijkl}(\boldsymbol{\xi},\mathbf{x})\sum_{I=1}^{n}\bar{\Phi}_I(\mathbf{x})\,\dot{\sigma}^p_{kl}(\mathbf{x}_I)\, d\Omega_d(\mathbf{x})\right)+ \\
&+g_{ij}\left(\dot{\sigma}^p_{kl}\right)
\end{aligned}
\tag{11}
$$

where *ne* is the total number of boundary elements of the model, *nnoel* is the number of element nodes, and *NT* is the number of triangular sub-domains used for effecting the domain integrations. By writing then Eqs. (10) and (11) for all boundary nodes and interior points, the systems of algebraic equations arise

$$\mathbf{H}\,\dot{\mathbf{u}} = \mathbf{G}\,\dot{\mathbf{p}} + \mathbf{Q}\,\dot{\boldsymbol{\sigma}}^p \tag{12}$$

$$\dot{\boldsymbol{\sigma}} = \mathbf{G}'\dot{\mathbf{p}} - \mathbf{H}'\dot{\mathbf{u}} + \mathbf{Q}^*\dot{\boldsymbol{\sigma}}^p \tag{13}$$

in which $\mathbf{Q}^* = \mathbf{Q}' + \mathbf{E}'$, the matrices $\mathbf{Q}$ and $\mathbf{Q}'$ result from the integration of plastic terms and $\mathbf{E}'$ corresponds to the free term $g_{ij}\left(\dot{\sigma}^p_{kl}\right)$.

After the application of the displacement and traction boundary conditions, Eqs. 12 e 13 can be written as

$$\mathbf{A}\,\dot{\mathbf{y}} = \dot{\mathbf{f}} + \mathbf{Q}\,\dot{\sigma}^p \tag{14}$$

$$\dot{\sigma} = -\,\mathbf{A}'\,\dot{\mathbf{y}} + \dot{\mathbf{f}}' + \mathbf{Q}^*\dot{\boldsymbol{\sigma}}^p \tag{15}$$

Solving Eq. 14 for the boundary unknowns, represented by the vector

$$\dot{\mathbf{y}} = \dot{\mathbf{m}} + \mathbf{R}\,\dot{\boldsymbol{\sigma}}^p \tag{16}$$

and substituting the result in Eq. 15 the expression

$$\dot{\sigma} = \mathbf{S}\,\dot{\boldsymbol{\sigma}}^p + \dot{\mathbf{n}} \tag{17}$$

is obtained.

In Eqs. 16 and 17, $\mathbf{R} = \mathbf{A}^{-1}\mathbf{Q}$, $\dot{\mathbf{m}} = \mathbf{A}^{-1}\dot{\mathbf{f}}$ (elastic solution of the boundary problem), $\mathbf{S} = \mathbf{Q}^* - \mathbf{A}'\,\mathbf{R}$ and $\dot{\mathbf{n}} = \dot{\mathbf{f}}' - \mathbf{A}'\,\dot{\mathbf{m}}$, in which the latter represents the solution in terms of stresses in absence of plasticity.

4 Constitutive equations

In plasticity the evaluation of the final state of stress and strain of a body depends on the loading history, i.e., the final deformation of the body is given by the sum of plastic strain increments throughout all the process. Therefore, it is convenient to write the stress–strain relationships incrementally as follows

$$\dot{\sigma}_{ij} = c^{ep}_{ijkl}\, \dot{\varepsilon}_{kl} \tag{18}$$

where $\dot{\varepsilon}_{kl}$ is the total strain increment and

$$c^{ep}_{ijkl} = c_{ijkl} - \frac{1}{\gamma'} c_{ijmn} a_{mn} a_{op} c_{opkl} \tag{19}$$

is the fourth–order elastoplastic tangent operator with:

$$c_{ijkl} = \frac{2G\nu}{1-2\nu}\delta_{ij}\delta_{kl} + G\left(\delta_{ik}\delta_{jl} + \delta_{il}\delta_{jk}\right) \tag{20}$$

$$a_{kl} = \frac{\partial F}{\partial \sigma_{kl}} = \frac{\partial \sigma_e}{\partial \sigma_{kl}} \tag{21}$$

$$\gamma' = a_{ij} c_{ijkl} a_{kl} + H' \tag{22}$$

and

$$H' = \frac{d\sigma_0}{d\varepsilon^p_e} \tag{23}$$

In the above equations c_{ijkl} is the fourth–order tensor of elastic constants, δ_{ij} is the Kronecker delta symbol, H' is the slope of the uniaxial stress–strain curve σ_0, σ_e is the equivalent or effective stress defined by the yield criterion and ε^p_e is the equivalent plastic strain.

Defining also an incremental fictitious "elastic stress", i.e.,

$$d\sigma^e_{ij} = c_{ijkl} d\varepsilon_{kl} \tag{24}$$

then, equation 18 can be rewritten as

$$d\sigma_{ij} = d\sigma^e_{ij} - \frac{1}{\gamma'} c_{ijmn} a_{mn} a_{kl} d\sigma^e_{kl} \tag{25}$$

From Eq. 25 it follows that the true stress increments can be computed from the "elastic stress" increments and the corresponding inelastic stress increments, which are given by

$$d\sigma^p_{ij} = d\sigma^e_{ij} - d\sigma_{ij} = \frac{1}{\gamma'} c_{ijmn} a_{mn} a_{kl} d\sigma^e_{kl} \tag{26}$$

If a similar procedure is adopted for the integral equations, the fictitious elastic stress increments can be directly evaluated by substituting the free term by

$$\bar{g}_{ij}\left(\dot{\sigma}_{kl}^{p}\right) = g_{ij}\left(\dot{\sigma}_{kl}^{p}\right) + \dot{\sigma}_{ij}^{p} \tag{27}$$

which is equivalent to replace the matrix $\mathbf{S}$ by $\bar{\mathbf{S}} = \mathbf{S} + \mathbf{I}$, where $\mathbf{I}$ is the identity matrix. Thus one can write

$$\boldsymbol{\Delta\sigma}^{e} = \bar{\mathbf{S}}\boldsymbol{\Delta\sigma}^{p} + \boldsymbol{\Delta}\mathbf{n} \tag{28}$$

5 Elastoplastic solution technique

In this work one adopts the explicit technique based on the application of Eq. 28 [Telles and Carrer (1988, 1991, 1994); Miers and Telles (2004)]. The incremental–iterative process starts with the reduction of the maximum equivalent stress ($\sigma_e^{\max}$), calculated considering the elastic solution of the problem, to the initial yield stress of σ_0, by the expression

$$\lambda_0 = \frac{\sigma_0}{\sigma_e^{\max}} \tag{29}$$

where λ_0 is the initial load factor.

The next load factor values are calculated by

$$\lambda_i = \lambda_{i-1} + \beta \tag{30}$$

with

$$\beta = \lambda_0 \omega \tag{31}$$

In Eq. 31 ω is the load increment value with respect to the load of first yielding and the incremental process ends when $\lambda_i = 1$. Thus, equations 16 and 17 can be applied as

$$\dot{\mathbf{y}} = \mathbf{R}\left(\dot{\boldsymbol{\sigma}}^{p} + \boldsymbol{\Delta}\dot{\boldsymbol{\sigma}}^{p}\right) + \lambda_i \dot{\mathbf{m}} \tag{32}$$

$$\dot{\boldsymbol{\sigma}} = \mathbf{S}\left(\dot{\boldsymbol{\sigma}}^{p} + \boldsymbol{\Delta}\dot{\boldsymbol{\sigma}}^{p}\right) + \lambda_i \dot{\mathbf{n}} \tag{33}$$

6 Applications

To illustrate how the technique proposed performs, three numerical examples are presented. It is worth mentioning that in every analysis has been adopted: a quadratic basis, a Gaussian weight function with the constant $c_i = 0.3\,r_i$ and the yield criterion of von Mises.

6.1 Perforated plate

In this example one has a perforated plate in plane stress state as presented in Fig. 3.

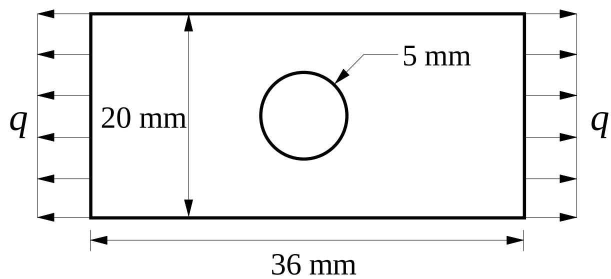

Figure 3: Perforated plate

The following problem data is considered: $E = 7000\ kgf/mm^2$, initial yield stress $\sigma_0 = 24.3\ kgf/mm^2$, $H' = 0.032E$ and $\nu = 0.2$. The applied load is $q = 11.5\ kgf/mm^2$ and the load increment is 10%.

Because of symmetry, only one quarter of the plate is discretized. Figure 4 shows the discretization used in this analysis, wherein *ne* is the number of boundary elements, *nc* is the number of cells, and *np* is the number of inner points. The plate was also analyzed with the Finite Element Method (FEM) using 2944 quadratic elements (PLANE183 – 8 node) to discretize the problem, as depicted in Fig. 4c.

The ratio between the σ_x–stress and the yield stress on points located over the y–axis is given in Fig. 5.

Fig. 6 shows the evolution of the plastic zone for different load levels.

6.2 Polystyrene under stress

In this example one studies the effect of voids in polystyrene strength. The geometry of the problem and its discretization are given in Figs. 7 and 8. Ideal plasticity was assumed with: $E = 4.2 \times 10^3\ MN/m^2$, initial yield stress $\sigma_0 = 105\ MN/m^2$ and $\nu = 0.33$.

Plane strain approximation and two loading conditions were considered: biaxial tension and uniaxial tension, both applied by prescribing displacements (Δ) at the edges. The displacement increment was 5%.

In Figs. 9 and 10, the mean stress (R) is plotted as a function of the applied displacement.

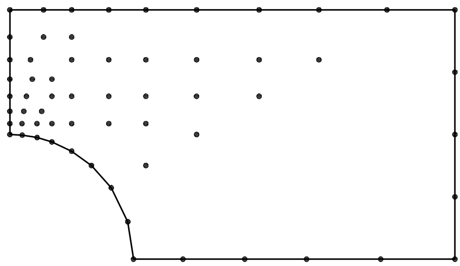

a) OMLS ($ne = 33$, $np = 28$)

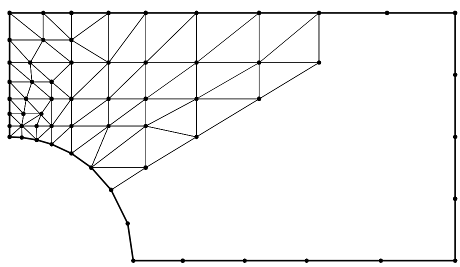

b) With cells ($ne = 33$, $nc = 71$)

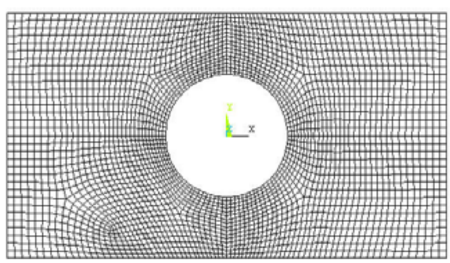

c) Finite element mesh

Figure 4: Discretization adopted

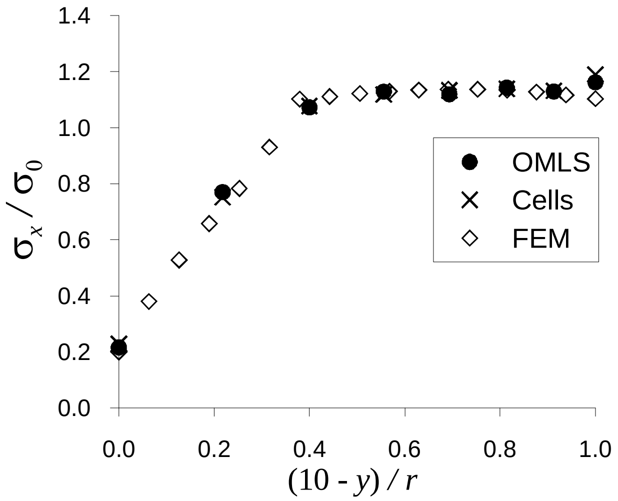

Figure 5: σ_x–stress at y–axis

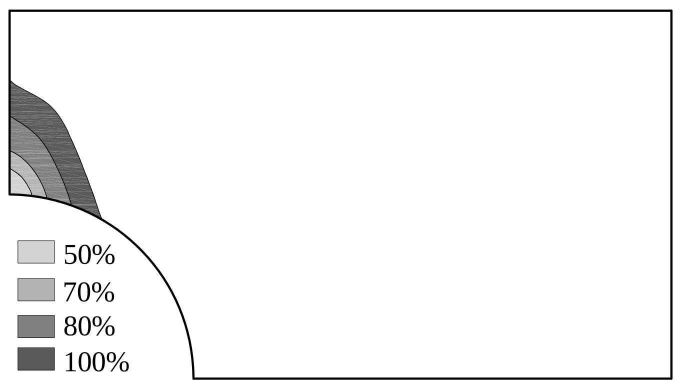

Figure 6: Plastic zones – Perfurated plate

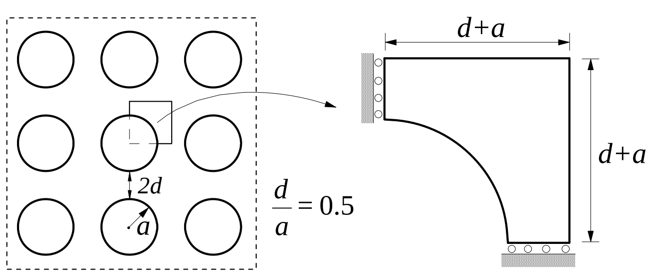

Figure 7: Polystyrene and the portion analyzed

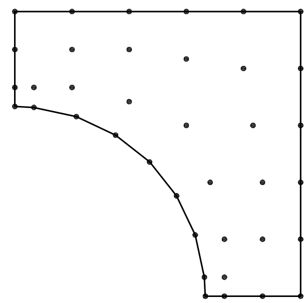

a) OMLS ($ne = 24$, $np = 14$)

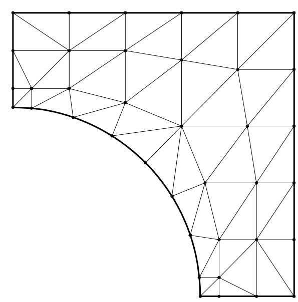

b) With cells ($ne = 24$, $nc = 50$)

Figure 8: Polystyrene discretization

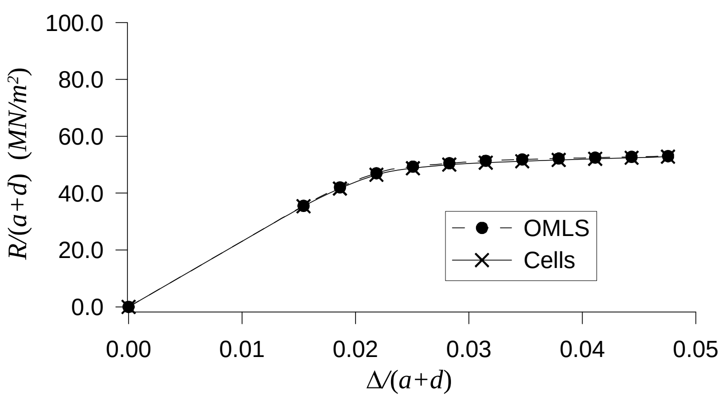

Figure 9: Mean stress vs. strain curve – uniaxial tension

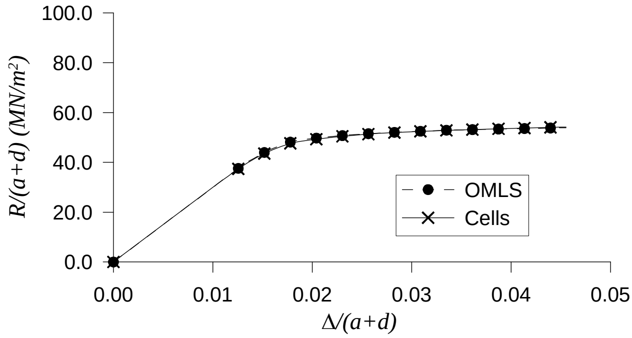

Figure 10: Mean stress vs. strain curve – biaxial tension

6.3 *Punch problem*

In this example one analyses a block compressed by two opposite rigid punches, as shown in Fig. 11, considering plane strain state.

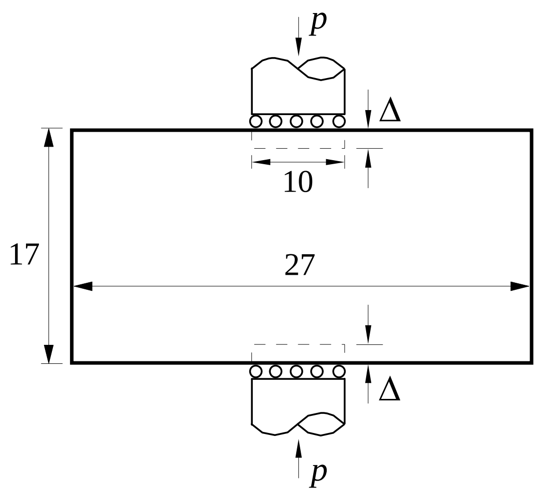

Figure 11: Plane strain punch problem

The physical properties of the material are: $E = 10^7\ psi$, initial yield stress $\sigma_0 = 13000psi$ and tangent modulus $E_T = 0$. The prescribed displacement, Δ, is 0.035” and it was adopted a displacement increment of 10%. The discretization of the problem is shown in Fig. 12.

The relation between the mean pressure applied by the rigid punch and its pre-

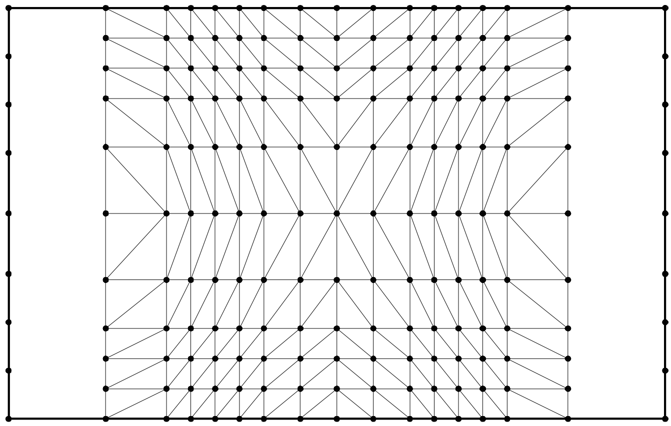

Figure 12: Punch problem discretization

scribed displacement is shown in Fig. 13, where b is the half–width of the rigid punch.

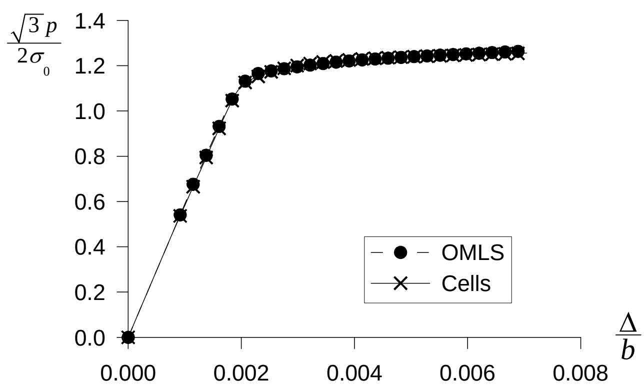

Figure 13: Mean pressure vs. displacement curve

In Fig. 14 one has the evolution of the plastic zone as the rigid punch compresses the block.

7 Conclusions

In this work, the OMLS interpolation technique has been employed to approximate residual plastic stresses present in boundary element formulations for inelastic problems. In this technique the function values at any point are reconstructed

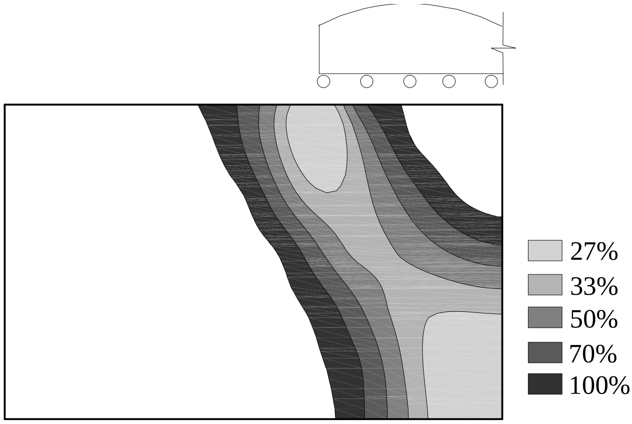

Figure 14: Plastic zones – Punch problem

from isolated points spread inside its definition domain. The excellent agreement observed in the comparison of results shows that OMLS can be regarded as an effective alternative to evaluate BEM domain integrals. Of course, an advantage of OMLS is to make the model generation considerably easier, without need to define cell connectivity, just the coordinates of the domain points.

Acknowledgement: This research was sponsored by the Brazilian Research Council (CNPq), and by the Research Foundation for the State of Minas Gerais (FAPEMIG).

References

Atluri, S. N.; Shen, S. (2002): The Meshless Local Petrov–Galerkin (MLPG) Method: A Simple & Less–costly Alternative to the Finite Element and Boundary Element Methods. *CMES: Computer Modelling in Engineering and Sciences*, vol. 3, no. 1, pp.11–51.

Atluri, S. N.; Shen, S. (2005): The Basis of Meshless Domain Discretization: The Meshless Local Petrov–Galerkin (MLPG) Method: *Advances in Computational Mathematics, Springer*, vol. 23, pp.73–93.

Atluri, S. N.; Zhu T. (2000): The Meshless Local Petrov–Galerkin (MLPG) Approach for Solving Problems in Elasto–Statics: *Computational Mechanics*, vol. 25, pp. 169–179. Springer–Verlag.

Brebbia, C. A., Telles, J. C. F. e Wrobel, L. C. (1984): *Boundary element techniques: theory and applications in engineering*. Springer–Verlag, Berlin.

Kreider, D. L.; Kuller, R. G.; Ostberg, D. R.; Perkins, F. W. (1966): *An Introduction to Linear Analysis,* vol. 2, Addison–Wesley Publishing Company Inc.

Liew, K. M.; Cheng, Y.; Kitipornchai, S. (2006): Boundary Element–Free Method (BEFM) and Its Application to Two–dimensional Elasticity Problems: *International Journal of Numerical Methods in Engineering*, vol. 65, no. 8, pp. 1310–1332.

Miers, L. S.; Telles J. C. F. (2004): A general tangent operator procedure for implicit elastoplastic BEM analysis: *CMES: Computer Modelling in Engineering and Sciences*, vol. 6, no. 5, pp. 431–439.

Telles, J. C. F. (1983): *The Boundary Element Method Applied to Inelastic Problems: Lecture Notes in Engineering*. vol.1, Berlin, Springer–Verlag.

Telles, J. C. F. (1985): On Inelastic Analysis Algorithms for Boundary Elements, Advanced Topics in Boundary Elements: *In: Cruse, T. A., Pifko, A. B. and Arnen, H., (eds.) Winter Annual Meeting of the ASME – AMD*, vol. 72, Miami, USA, pp. 35–44.

Telles, J. C. F.; Carrer J. A. M. (1988): Implicit Solution Techniques for Inelastic Boundary Element: *10th BEM*, vol. 3, pp. 3–15.

Telles, J. C. F.; Carrer J. A. M. (1991): Implicit Procedures for the Solution of Elastoplastic Problems by the Boundary Element Method: *Mathematical Computational Modelling*, vol. 15, no. 3–5, pp. 303–311.

Telles, J. C. F.; Carrer J. A. M. (1994): Static and Transient Dynamic Nonlinear Stress Analysis by the Boundary Element Method with Implicit Techniques: *Engineering Analysis with Boundary Elements*, vol. 14, no. 1, pp. 65–74.